ROMANIAN ACADEMY
SCHOOL OF ADVANCED STUDIES OF THE ROMANIAN ACADEMY
INSTITUTE OF BIOCHEMISTRY

PH.D. THESIS SUMMARY

Bioinformatics analyses of pharmaco-genomic networks as methods to study lifespan modulation

Ph.D. Student:
Gabriela Bunu

Scientific coordinator:
Dr. Andrei-José Petrescu

Bucharest
2023

Contents

1. Background and scope..... 2
2. Results and discussion..... 3
2.1. Proposed definitions for synergism..... 3
2.2. The SynergyAge database..... 8
2.3. Network models in longevity..... 12
2.4. Meta-analysis of the aging signature..... 15
2.5. Age-related diseases and age-associated processes..... 16
2.5.1. Consensus transcriptional profile in the AD-Cluster and PD-Cluster..... 18
2.5.2. Pulmonary fibrosis..... 18
2.6. Drug repurposing..... 21
2.6.1. Drugs with potential to reverse the shift in transcriptional profile associated with neurodegenerative diseases..... 21
2.6.2. Small molecules for cell reprogramming..... 22
2.6.3. Drugs that induce pluripotency as potential agents against neurodegenerative pathologies..... 25
3. Final remarks..... 27
List of publications and presentations..... 29
Bibliography..... 31

1. Background and scope

Aging is a complex and multifactorial process that leads to a loss of viability and an increased frailty. It is also the major risk factor for many age-related diseases, such as Alzheimer's disease, Parkinson's disease, cancer and cardiovascular diseases. As the population distribution changes and the proportion of elderly people in society increases, the increased healthcare cost in old age can become a burden on the healthcare system.

When referring to the aging process, there are two important concepts: i) lifespan, which defines the length of time that a person or animal lives, and ii) healthspan, which defines the length of time that an organism spends in a healthy state. In the last decades, human life expectancy has increased dramatically, but the healthspan did not follow the same magnitude of change (Ge et al., 2022). Generally, aging research aims to increase the healthspan, in order to significantly reduce the occurrence of age-related diseases with the ideal goal of identifying treatments or therapies that ensure a longer, but also healthier life in humans (DeVito et al., 2022). Yet, the current paradigm of treatment when referring to age-related diseases is still to consider each disease separately, without focusing on the main cause, which would be aging itself (Blagosklonny, 2012).

One of the major challenges in understanding aging is identifying its underlying molecular and cellular mechanisms. For example, a plethora of genes are known to be involved in lifespan determination, aging processes, as well as in age-related diseases. Similarly, at an epigenetic level, more and more regulating mechanisms have been uncovered. Nevertheless, putting all these data together in order to fully model the aging process or its intimate relationship with various pathologies is still eluding. Still, recent advances in bioinformatics have provided new opportunities to study aging and age-related diseases at the systems level (Xue et al., 2007; Fernandes et al., 2016; Miller et al., 2008; Tacutu et al., 2011; Zhang et al., 2016). Among these novel methodologies, bioinformatic analyses of mixed drug-gene networks can provide some unique new insights into the biological processes that underlie aging and age-related diseases (Fuentealba et al., 2019; Xie et al., 2022; Liu et al., 2016). More importantly, these analyses allow for the integration of multi-model data and the identification of novel targets and pathways, through functional relationships between genes and drugs, thus steering research towards novel treatments and therapies.

This work aims to explore such bioinformatic analyses, in order to identify: i) genetic and transcriptional signatures of aging and age-related diseases, ii) potential targets

for therapeutic interventions that can delay the onset or progression of age-related diseases, and iii) potential approved drugs that can be repurposed as longevity modulators. This research will contribute to our understanding of the complex biological processes that underlie aging and aims to have important implications for drug repurposing in age-related diseases.

2. Results and discussion

2.1. Proposed definitions for synergism

Many perturbation studies have shown that aging is a process that can be genetically modulated. Despite hundreds of single-gene interventions being known thus far, looking at individual interventions might not give a broad enough view of the regulatory mechanisms of the aging process. However, genes do not interact in a simple, linear way, thus being difficult to predict the outcome of combining two or more interventions. Because of the complex interactions between two or multiple genetic interventions, I proposed new comprehensive definitions for assessing their outcome.

In order to assess the effect of a combination of two interventions, four lifespan values have to be determined, for the following strains: wild type, single mutants G1 and G2, as well as the double mutant G1;G2. The effect of each mutant is defined as the percentage of change in lifespan compared to the wild-type lifespan, as follows:

$\Delta G1 = (LS(G1) - LS(WT)) * 100 / LS(WT)$

$\Delta G2 = (LS(G2) - LS(WT)) * 100 / LS(WT)$

Next, the effect of a combination of interventions with same directionality ($\Delta G1*\Delta G2 >0$) was defined as follows (see also Fig. 1 and Fig. 2):

- **fully synergistic**, if $|\Delta(G1,G2)| > |\Delta G1| + |\Delta G2|$ (Fig. 2A, B)
- **additive**, if $|\Delta(G1,G2)| \cong |\Delta G1| + |\Delta G2|$ (Fig. 2C, K)
- **almost additive**, if $|\Delta(G1,G2)| > \max(|\Delta G1|, |\Delta G2|)$ and $|\Delta G1,G2| < |\Delta G1|+|\Delta G2|$ (Fig. 2D, E)
- **antagonistic, dependent**, if $|\Delta G1,G2| < \max(|\Delta G1|, |\Delta G2|)$ and $|\Delta G1,G2| > \min(|\Delta G1|, |\Delta G2|)$ (Fig. 2H)
- **fully antagonistic**, if $|\Delta G1,G2| < \min(|\Delta G1|, |\Delta G2|)$ (Fig. 2F, G)

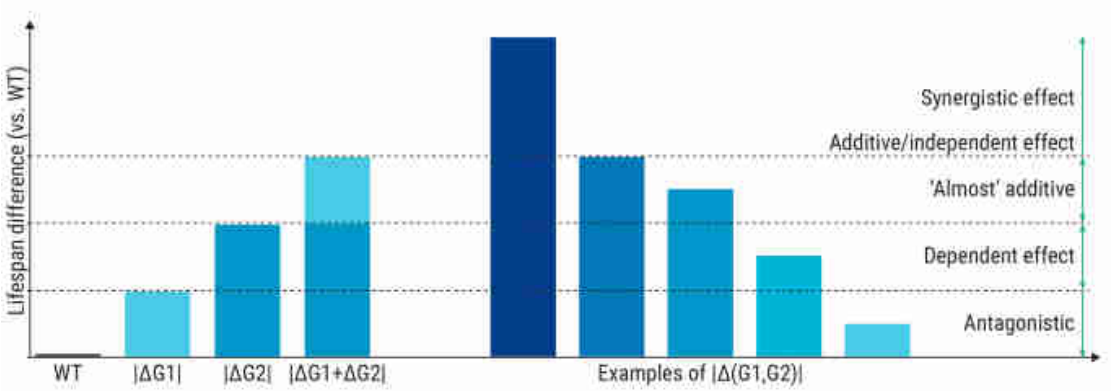

Figure 1. Types of interactions for a double mutant with the same direction for single gene intervention effects. The bars on the left represent the absolute value of the effect on lifespan of each intervention, compared to wild type. The sum of the effects is shown for reference. The bars on the right represent examples of each type of combination: synergistic, additive, almost additive, dependent and antagonistic. Figure derived from (Bunu et al., 2020), used under license CC BY 4.0.

Monotony

Given that in general not all possible mutants are assessed in a lifespan study, monotony can be evaluated instead of full synergism. This type of analysis involves identifying all paths from wild type to the n-mutant ($n \geq 2$), where a path represents a sequence of n+1 strains, starting from wild type and adding at each step k the mutant constructed from the (k-1) mutant, e.g. a path could be wild type -> G1 -> G1;G2 -> G1;G2;G3. If the direction of change is consistent through each mutant in a path, i.e. each k-mutant increases the lifespan of the (k-1) mutant, or each k-mutant decreases the lifespan of the (k-1) mutant, then a path is considered monotonic. If all the identified paths are monotonic (according to all experimental observations in a study), then the n-mutant has a monotonic epistatic interaction (Fig. 2M, N). Otherwise, if at least one path does not meet the monotony criteria, then the n-mutant contains some dependencies amongst its n components (Figure 2L).

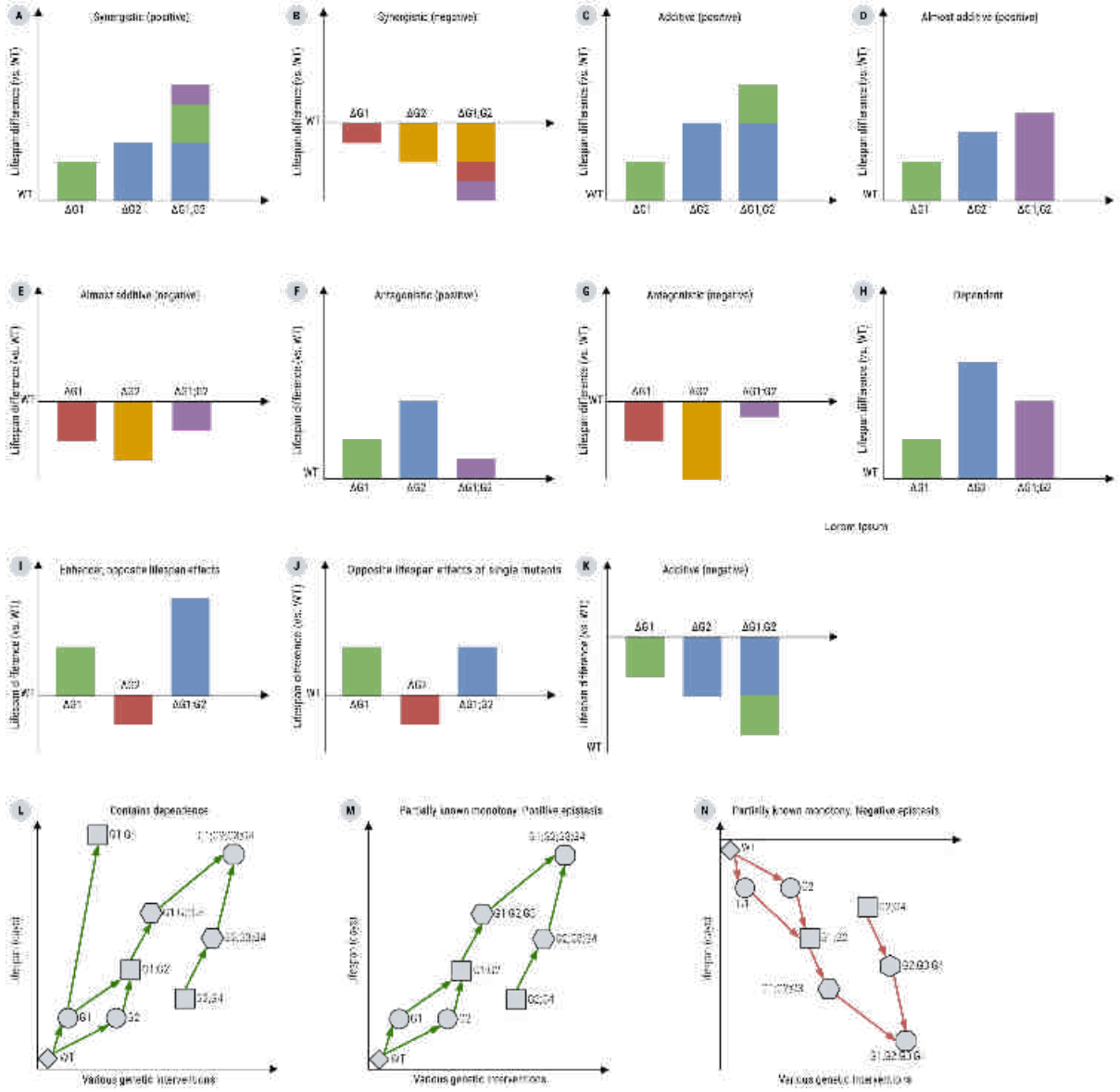

Figure 2. Graphical representation of all the categories of effects between two or more genetic interventions assessed in SynergyAge. A-J. The bars represent the effects of each intervention (ΔG1 and ΔG2) and the effect of the combination (ΔG1;G2), as a percentage compared to wild type. **A.** Example of positive synergism - the effect of the combination is larger than the sum of individual effects. **B.** Example of negative synergism - the absolute value of the effect of the combination is larger than the sum of absolute values of individual effects. **C.** Example of positive additive effect - the effect of the combination is approximately equal to the sum of individual effects. **D.** Example of almost additive positive effect - the effect of the combination is greater than any of the two individual effects but smaller than their sum. **E.** Example of almost additive negative effect - the absolute value of the effect of the combination is greater than any of the two absolute values of individual effects, but smaller than their sum. **F.** Example of positive antagonistic effect - the effect of the

combination is smaller than any of the two individual effects. **G.** Example of negative antagonistic effect - the absolute value of the effect of the combination is smaller than any of the two absolute values of individual effects. **H.** Example of dependent relationship - the effect of the double mutant (G1, G2) is larger than the effect of G1, but smaller than the effect of G2. **I.** Example of enhancer (G2) with opposite lifespan effect - the effect of the combination is larger than the effect of the single mutant G1, even though G2 has a negative effect. **J.** Example of combination with opposite effects for the single interventions. **K.** Example of additivity for negative effects - the absolute value of effect of the combination is approximately equal to the sum of the absolute values of individual effects. **L.** Example of n-mutant containing dependence - G1;G4 is longer lived than G1;G2;G3;G4 mutant. **M.** Example of partially known monotony (positive epistasis). **N.** Example of partially known monotony (negative epistasis).

Synergism for n-mutant

As expected, the cumulative effects of n-component interactions are more difficult to define for combinations of 3 or more interventions. The most common definition for synergism is "greater than the sum of its parts", i.e. $\Delta|G1,G2,...Gn| > |\Delta G1| + |\Delta G2| + \ldots.+ |\Delta Gn|$ (Fig. 3B), however, this definition might not be appropriate to use for complex genetic interactions. Fig. 3C shows a hypothetical example of how it can be misleading: the individual interventions are in agreement with the aforementioned hypothesis of "greater than the sum of its parts", but there are two double mutants (G1;G2 and G1;G3) with a longer lifespan than the triple mutant G1;G2;G3. In this case, we can state that interventions G1 and G2 are synergistic, but this increase in lifespan is dependent on gene G3 being intact/unaffected (i.e. without mutations, silenced, overexpressed, etc). In fact, this is a case of dependent interaction, according to the definitions proposed in this work (see above).

On the other hand, for an n-mutant G1;G2;G3;…Gn, a "full" synergism" would mean that all the pairs (G1;G2…;Gk and Gk+1;Gk+2..;Gn) are synergistic themselves, i.e. ΔG1;G2;G3…Gn > ΔG1;G2…;Gk + ΔGk+1;Gk+2..;Gn. (Fig. 3A). In order to assess this type of synergism, all the n! (n factorial) lifespan values have to be determined, and unfortunately, in practice, this would represent an intensive wet lab effort and is often out of the scope of lifespan studies.

Because of the lack of experimental data, I proposed another type of synergism: partially known monotonical synergism (Fig. 2M, N, Fig. 3D). In this case, it is possible that one or more paths are known, for example: 1) WT -> G1 -> G1;G2 -> G1;G2;G3 and 2) WT

-> G2 -> G2;G3 -> G1;G2;G3. A sequence of this type where each "step" has a higher lifespan than the previous mutant was defined as a monotonic path (see Monotony). If all the paths investigated have this property, then the effect of the n interventions represents a partially known synergism (Fig. 3D). Otherwise, the interaction relationship contains dependencies (Fig. 3E).

Antagonism for an n-mutant was defined in a similar manner and involves "full antagonism", partially known monotonic or simple antagonism.

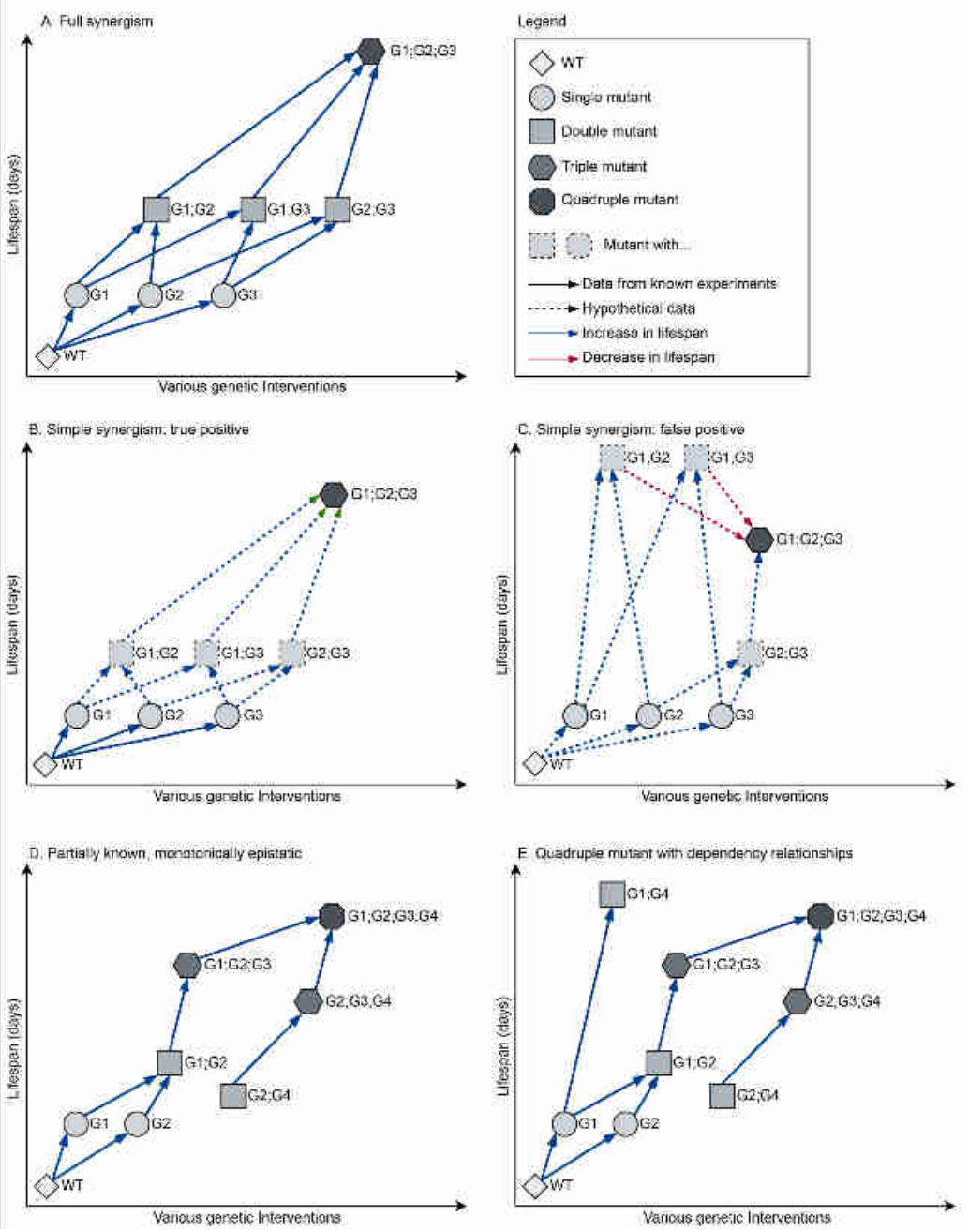

Figure 3. Representation of various types of synergism for n-mutants with at least two interventions. A. Example of full synergism between three interventions. **B.** Example of true

positive in the case of simple synergism assessment for three interventions. **C.** Example of false positive in the case of simple synergism assessment for three interventions: it meets the criteria for simple synergism, but it contains a dependency relationship (i.e., the magnitude of lifespan extension obtained with G1;G2 or G1;G3 depends on G3 and G2 respectively being unmodified - otherwise the effect decreases). **D.** Example of partially known, monotonically epistasis between four interventions. **E.** Example of quadruple mutant with dependency relationships. Figure derived from (Bunu et al., 2020), used under license CC BY 4.0.

2.2. The SynergyAge database

The focus of the SynergyAge database was to host studies that show either long- or short-lived mutants with at least two concomitant genetic interventions. SyngergyAge was built with manually curated data from the scientific literature.

The SynergyAge database contains almost 7,000 lifespan values for three model organisms: *C. elegans, D. melanogaster* and *M. musculus* (Table 1). The largest part of the available data was collected from worm experiments, because *C. elegans* is the most studied model for longevity, due to its short lifespan and environmental conditions requirements.

Table 1. Number of records in the SynergyAge database.

	C. elegans	***D. melanogaster***	***M. musculus***	**Total**
Lifespan values	6,656	185	147	6,988
Gene combinations (reported in studies)	1,770	27	3	1,833
Genes with at least 1 record	714	36	44	794
Articles	144	20	29	193

The web interface provides a network visualization for each model organism and multiple searching and filtering options (Figure 4).

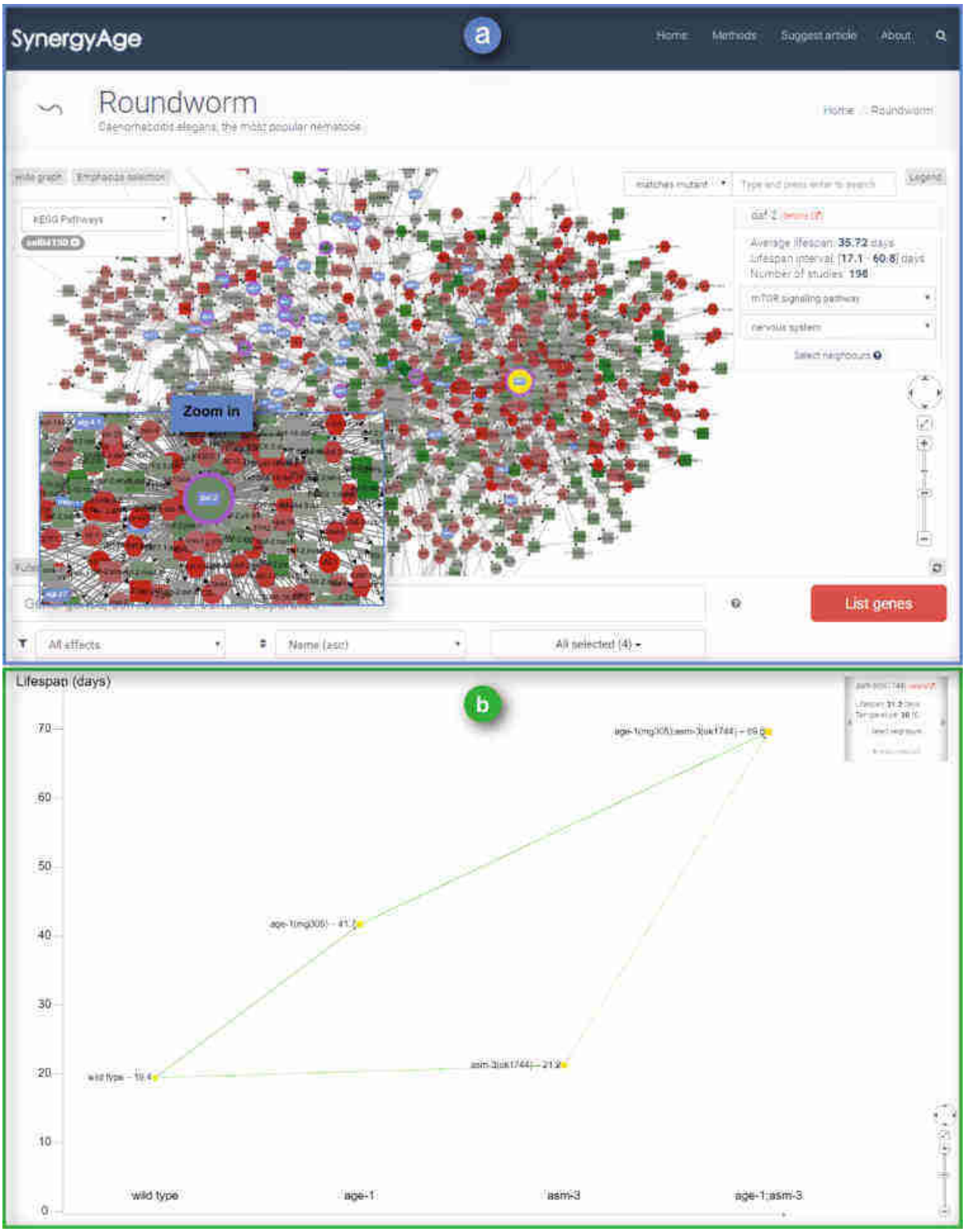

Figure 4. Network visualizations in the SynergyAge website. (a) Network visualization of the worm mutants. Each node represents a mutant (or wild type) and summarizes all its entries in the database (see the panel in the upper right). The color gradient codes its average effect compared to wild type - green for positive effects, red for negative effects, and grey for small effects. The node size is proportional to the number of records in the database. Edges are

drawn from an n-mutant to an (n+1)-mutant: solid lines are used for comparisons that were studied experimentally and dashed lines for inferred comparisons. In this example, the purple border corresponds to genes that belong to the selected pathway (cel04150, upper left panel) (b) Network visualization of the double mutant *age-1;asm-3*. Each node represents a cohort; edges were drawn only between cohorts studied in the same experiment. Green edges represent an increase in lifespan obtained with the additional intervention, whereas red edges depict interventions that determine a shorter-lived phenotype. Figure derived from (Bunu et al., 2020), used under license CC BY 4.0.

In order to propose a combination of interventions for experimental validation, we used the curated data to select genes that are at least almost additive with *daf-2,* to increase the probability of identifying gene combinations that are independent of the *daf-2*/insulin pathway. For all the pairs of genes from the initial list, we computed: a) the number of common KEGG pathways between them and b) whether they pertain to the same cluster in the embeddings provided by a machine learning model developed in our lab.

The initial prediction list included 25 candidate genes and 9 candidate combinations, each of them involving three genes. After an additional manual evaluation and literature research, we selected 3 combinations that were tested in a pilot experiment by my colleagues in the lab. After the pilot experiment, the combination of *odr-3;ife-2;cku-70* was selected for further testing, in more rigorous experiments.

The three genes selected for experimental validation were tested in longevity experiments in the nematode *C. elegans*, in all possible combinations and their effect was compared to single gene interventions and the wild type. Consistent with previous data, *odr-3* mutation and RNA interference in *ife-2* increased the mean lifespan compared to wild type by 26.2% and 18%, respectively (Fig. 5, Fig. 6). The increase in mean lifespan of *odr-3(n1605);ife-2(*RNAi) mutants compared to wild type was 40.3%, which represents an additive effect, because the effect of the double intervention is close to the sum of the two individual effects (44.2%). In the case of RNAi with a 1:1 mixture of empty vector (EV) bacteria and *ife-2* RNAi clone, the combination was synergistic: the increase in mean lifespan was 46.1% and the sum of the two individual effects was only 37.4%. RNAi in *cku-70* did not further extend the lifespan of the double mutant (Fig. 5, Fig. 6).

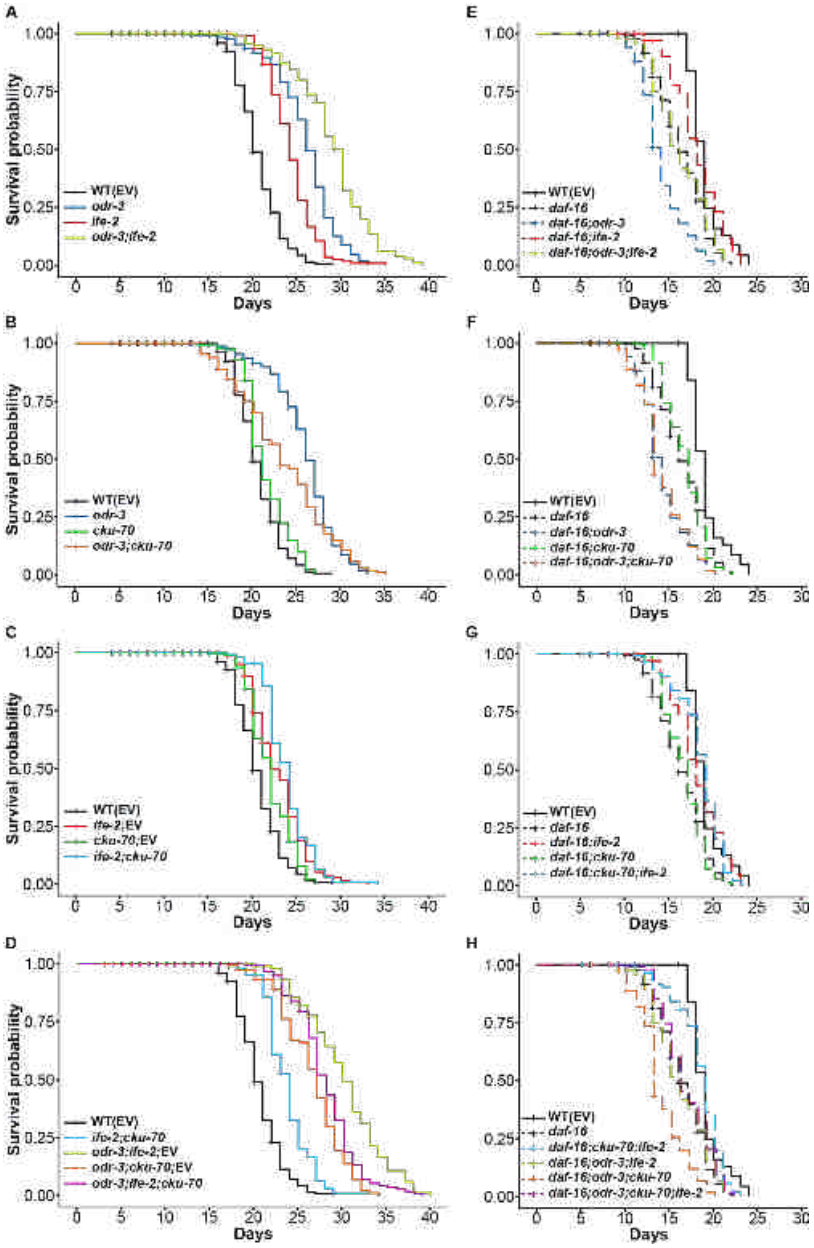

Figure 5. Kaplan-Meier survival curves depicting the effects of genetic interventions on *odr-3*, *ife-2,* and *cku-70*. A-D. The effects of single, double and triple interventions compared to wild type. **E-H**. The effects of single, double and triple interventions in the *daf-16(m26)* background. In the case of single RNAi knock-downs, the control is treated with a 1:1 mixture of RNAi and EV bacteria. Three independent experiments were performed in the wild type background and two independent experiments in the *daf-16* background. The plots represent the pooled populations from these experiments. *odr-3* represents the *odr-3(n1605)* mutant and *daf-16* represents the *daf-16(m26)* mutant; both mutants have been fed with EV. Figure derived from (Matei et al., 2021), used under license CC BY 3.0.

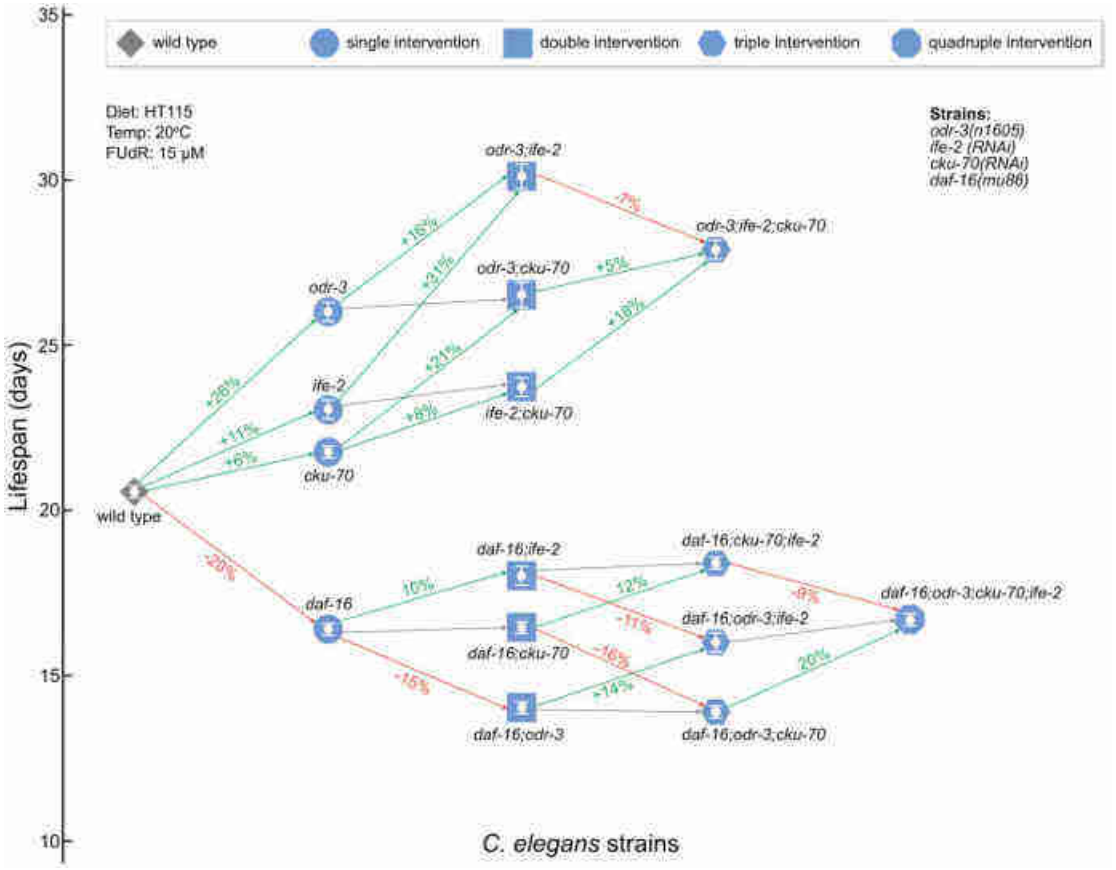

Figure 6. Network representation of the mean lifespans of each strain. Each node represents a strain (diamond - wild type, circle - single interventions, square - double interventions, hexagon - triple interventions and octagon - quadruple interventions) and its position on the y-axis is given by its mean lifespan. Edges connect n-mutants to (n+1)-mutants and quantify the effect of the (n+1) intervention as percentage compared to the n-mutant: green for increase, red for decrease and gray for non-significant effect in mean lifespan. *odr-3* represents the *odr-3(n1605)* mutation; *daf-16* represents the *daf-16(mu86)* mutation; *ife-2* denotes *ife-2*(RNAi) and *cku-70* denotes *cku-70*(RNAi). The bars inside the nodes represent the mean ± SEM. Figure derived from (Matei et al., 2021), used under license CC BY 3.0.

2.3. Network models in longevity

In the last decades, biological research shifted from reductionist approaches to holistic ones, as the field of system biology emerged. The holistic approach consists of analyzing the system as a whole, instead of individual components and often involves networks of interactions between molecular components. In this work, I modeled mixed networks of longevity-related proteins and drugs in order to explain the aging mechanisms from a systems biology perspective.

Data sources

The lists of genes and drugs already known to modulate the aging process were downloaded from the following public databases: i) GenAge (build 20) (Tacutu et al., 2018) - genes that determined a lifespan increase/decrease, when modified by an intervention (mutation, overexpression, RNA interference etc) in model organisms, also known as longevity associated genes (LAGs) and ii) DrugAge (Barardo et al., 2017) - molecules that showed a significant increase/decrease in lifespan when administered to model organisms. The list of molecules that are involved in inducing pluripotency was manually curated by our collaborators (Ben-Gurion University of the Negev, Israel) from the scientific literature.

Data for drug-protein interactions were retrieved from STITCH (Szklarczyk et al., 2016), using an in-house developed Python script, to query the database for relevant interactions. Only “database” and “experimental” evidence with at least medium confidence were used, excluding “text mining” and “prediction”.

Protein-protein interactions (PPIs) were integrated from BioGRID 3.5 (Oughtred et al., 2019) and only physical interactions were considered for further analysis. A summary table of counts for each of the data sources is included in Table 2.

Table 2. Summary statistics for the data selected for use in this work

Dataset	**Data type**	**Organism(s)**	**Number of records**	**Number of unique IDs**
GenAge	genes	*C. elegans*	1050	876
DrugAge	drugs	*C. elegans*	659	283
SMs involved in induced pluripotency	drugs	*H. sapiens*	92	92
BioGRID	genes/proteins	*C. elegans*	6069	6069

Longevity-associated genes form a network with a large connected component containing 253 nodes (44% of LAGs) - the "longevity network" (Fig. 7A). When taken together with their first-order partners, the percentage of nodes in the main connected component increases to an outstanding value of 95% of the network ("extended longevity network") (Fig. 7B). Together, these results show the cooperative nature of LAGs. LAGs are overrepresented among the proteins highly connected in the interactome (GSEA, NES = 1.28, p = 8.4e-15), suggesting their involvement in a large variety of processes. Interestingly, LAGs' partners are also among the most connected proteins (GSEA, NES = 1.45, p=2e-50) and the

difference in global connectivity within the BioGRID physical PPI network between LAGs and partners is not statistically significant (t-test, p=0.12). In fact, the top 372 most connected proteins in BioGRID belong to LAGs or their partners and 489 out of the top 500 most connected proteins are LAGs or their partners.

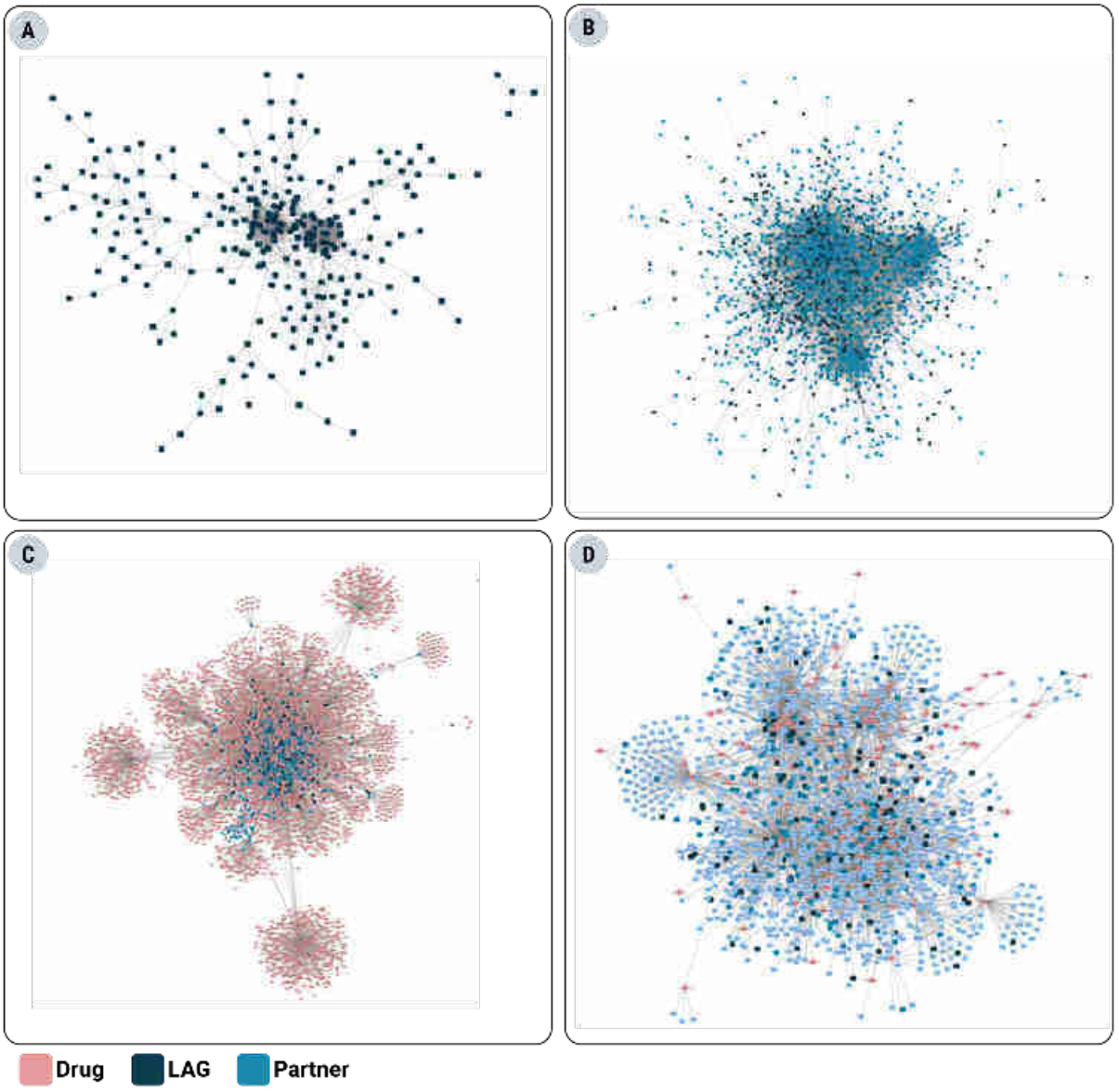

Figure 7. **Network models of longevity genes and drugs A**. Protein-protein interactions between LAGs; **B.** Extended longevity network (LAGs and their first order partners); **C.** Mixed network including LAGs, their first order partners and drugs that target them; **D.** Network of DrugAge drugs and their gene targets, including protein-protein interactions.

2.4. Meta-analysis of the aging signature

Another complementary approach to better understand the aging process at a more systems-wide perspective is to identify sets of molecular markers associated with age or an "aging signature", thus characterizing or assaying the entire system based on multiple molecular measurements. Several studies have used transcriptomic data from various tissues to identify such signatures and to investigate their association with age-related diseases and mortality. However, different technologies and preprocessing/analysis methods can generate variable results.

In this study, we used 5 aging-related datasets from *C. elegans* and 24 aging-related datasets from *H. sapiens*, downloaded from the GEO database and re-analyzed locally using in-house developed R scripts, in order to identify a common aging signature. Meta-analysis of old vs young datasets in *C. elegans* revealed a gene signature enriched for metabolic processes, longevity regulation and immune response.

Differentially expressed genes (DEGs) overlap significantly with the first order partners of LAGs, suggesting that the modulatory mechanisms of aging (represented by LAGs) and the mechanisms affected by the aging process (represented by DEGs) are not identical, but are very well interconnected.

Meta-analysis of human datasets showed that expression differences vary dramatically between different tissues (Fig. 8). However, for genes that change their expression in multiple tissues, in most cases the direction of these changes is the same (Fig. 9). In other words, if a gene is differentially expressed with age, its expression increases or decreases concordantly in all affected tissues.

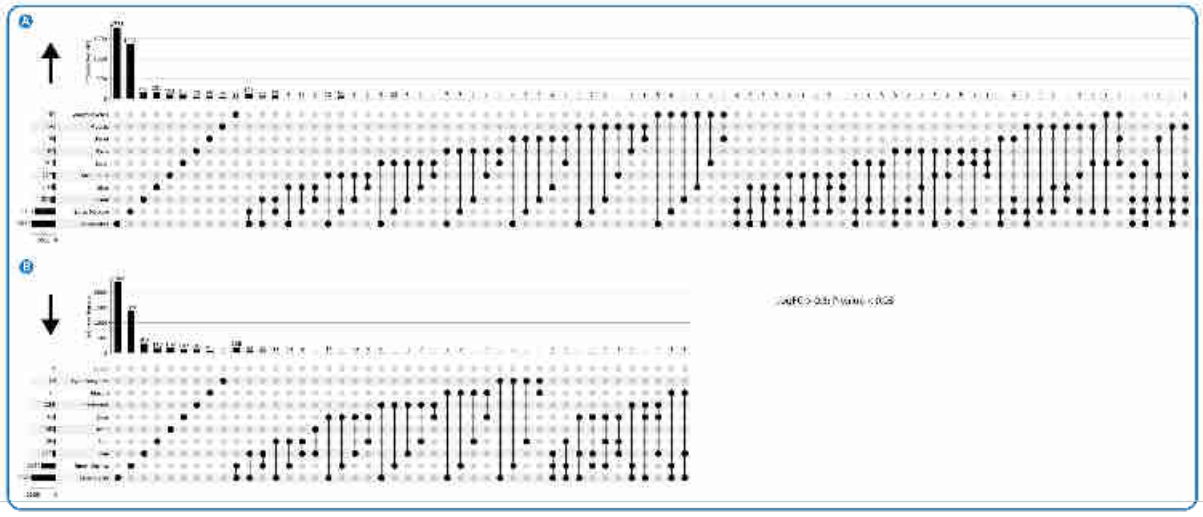

Figure 8. **Common or unique changes in gene expression in different tissues. A.** Genes upregulated during aging. **B.** Genes downregulated during aging. **A-B**. The number of up- or

downregulated genes in each tissue is shown in the bottom left; at the top are presented in a histogram the number of genes expressed in the same way in one or more tissues. For this analysis, the cutoff was set at LogFC > 0.5 and p-value < 0.05.

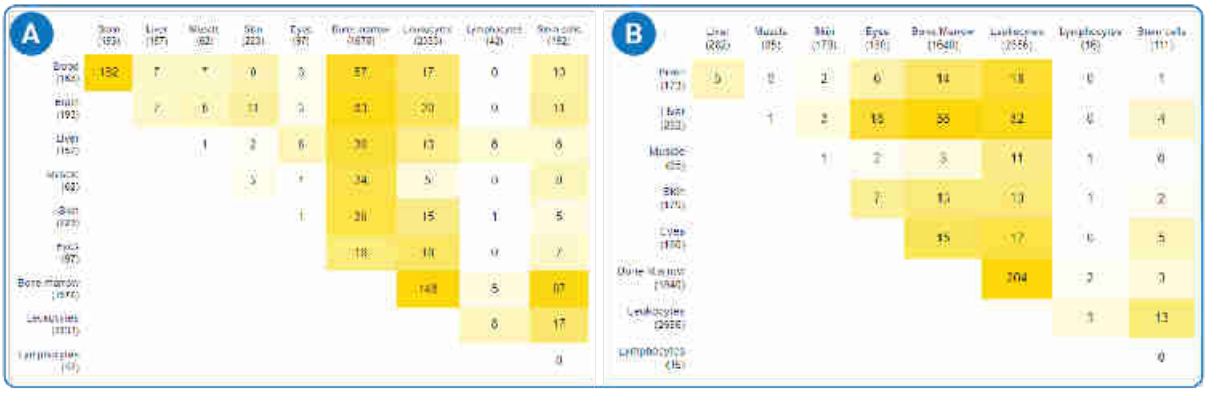

Figure 9. A. Up-regulated genes overlap between tissues old vs young. **B.** Down-regulated genes overlap between tissues old vs young.

2.5. Age-related diseases and age-associated processes

Because it is known that aging and age-related diseases share at least some degree of common mechanisms (Fernandes et al., 2016), a bioinformatics analysis was conducted in order to identify the potential common signature between the transcriptomic profiles of aging and ARDs. The following pathologies were selected: atherosclerosis, diabetes mellitus type II, Alzheimer's disease (AD), Parkinson's disease (PD) and osteoporosis.

I computed the similarity scores between each pair of transcriptional profiles using GSEA and the scores were visualized as a network consisting of 94 nodes (i.e. gene expression comparisons) and 826 edges (i.e. similarity scores). Using the MCL algorithm, the network in Fig. 10a was clustered and 4 clusters were obtained, of different sizes, plus a series of unconnected nodes (Fig. 10b).

Among these, two clusters stood out (Fig. 10b1, b2), presenting a greater number of connections between the nodes in their composition. The first cluster is focused on comparisons specific to neurodegenerative diseases (predominantly Alzheimer's) and on aging comparisons (predominantly in brain regions, but also blood) - which denotes certain specific mechanisms of brain aging - highly relevant to neurodegenerative diseases. Thus, I refer to the first cluster as the AD-Cluster. It contains 21 nodes, including 14 aging comparisons and 6 AD vs control comparisons, 94% of them sharing positive similarity scores, which shows a high consensus.

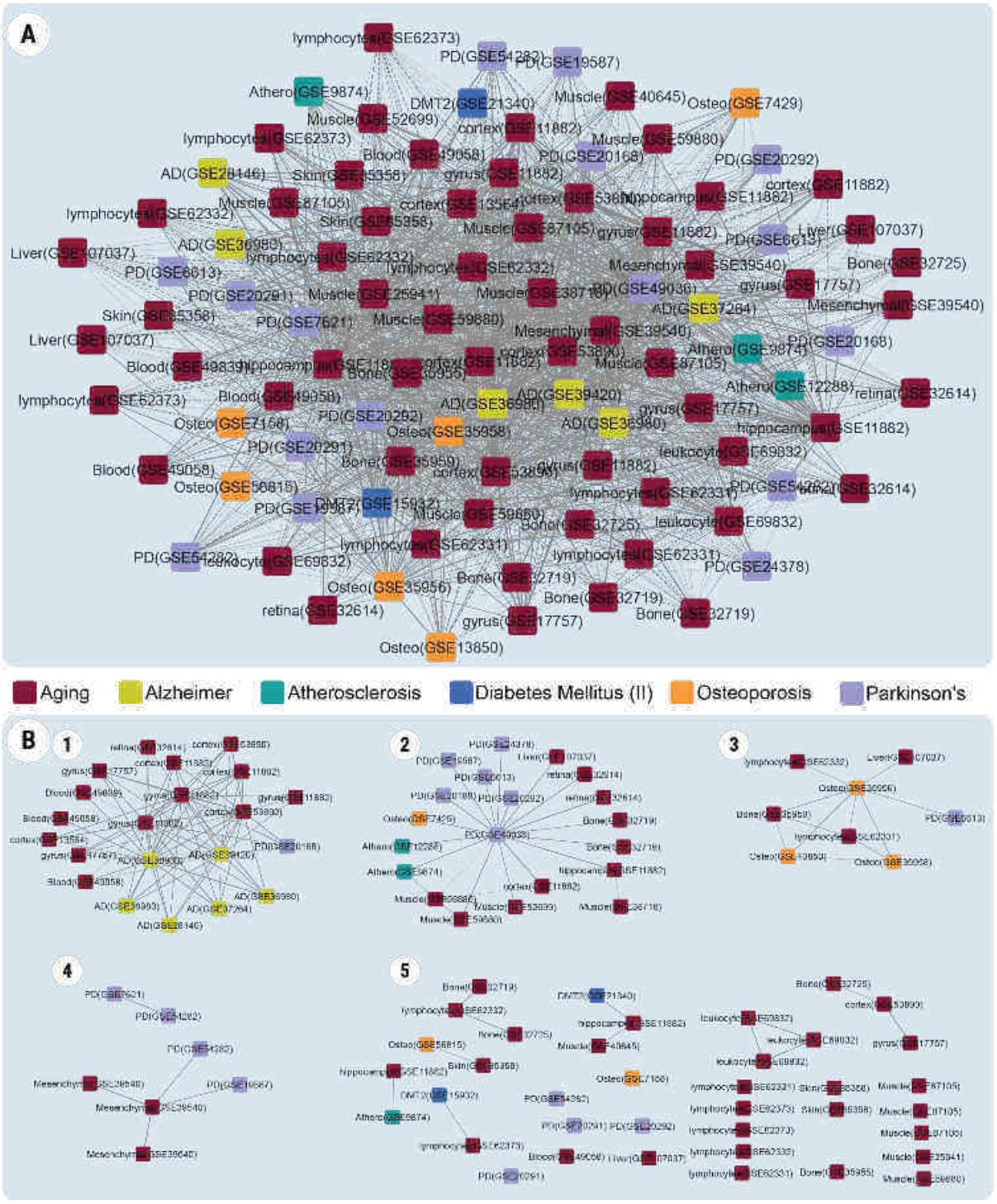

Figure 10. A. Undirected similarity network of the datasets from the targeted search (all diseases). **B.** Clusters obtained after applying the MCL algorithm to the network in panel A. **A-B.** The networks include the following comparisons type: 1) "healthy" aging (elderly vs. young) - red; 2) Alzheimer pathology - yellow; 3) Parkinson's pathology - purple; 4) atherosclerosis - turquoise; 5) Diabetes Mellitus type 2 - blue; 6) osteoporosis - orange. For simplicity, comparisons are shown only using the data set name (GSE); each node represents a

comparison between two states/conditions analyzed in each study. Interactions between nodes represent similarity scores between two comparisons, higher than a threshold. Positive similarity scores are represented by a solid line; negative scores are represented by a dotted line.

The second cluster is more characteristic of Parkinson's disease (6 comparisons), but also includes age-related changes and, interestingly, profiles of osteoporosis (1 comparison) and atherosclerosis (2 comparisons) as well. The tissues represented for aging comparisons are diverse and include brain, bone, muscle, liver and retina. I further referred to this cluster as the PD-Cluster.

2.5.1. Consensus transcriptional profile in the AD-Cluster and PD-Cluster

In order to identify the common changes in transcriptional profiles for aging and age-related diseases, we performed two separate meta-analyses, for AD-Cluster and for PD-Cluster. For each of them, because we wanted to prioritize the consistency of direction rather than the strength of change, we selected only the significant genes in each dataset (p value<0.05) that have consistent direction in all datasets and a fold change greater than 2 in at least one comparison.

Enrichment analyses revealed that the upregulated genes in the AD-Cluster are enriched for processes related to wound healing, cytokine production, stress response to copper ion and vascular development, while the downregulated genes were enriched for axon development, synaptic transmission and transmembrane transport. The PD-Cluster upregulated genes are enriched for protein sumoylation, photoreceptor cell differentiation, response to growth factor stimulus and the downregulated genes are enriched for fatty acid transport and maintenance of synapse structure.

2.5.2. Pulmonary fibrosis

Besides major ARDs, there are many other, perhaps less in the headlines, diseases and processes, with a high societal cost and major consequences on the organism, such as pulmonary fibrosis. Tissue fibrosis is a process whose incidence increases with age. Several organs can be affected, the lungs being one of the most susceptible.

In this work, a list of 212 non-redundant mouse genes was curated and divided into three categories: pro-fibrotic (50%), anti-fibrotic (43.5) and inconsistent (6.5%), i.e., showing both pro- and anti-fibrotic evidence. A pro-fibrotic gene represents a gene that increases

fibrosis when overexpressed and/or reduces fibrosis when downregulated. Similarly, an anti-fibrotic gene is a gene that increases fibrosis when downregulated and/or decreases fibrosis when overexpressed. These genes are referred to as pulmonary fibrosis-related genes (PFRGs).

Enrichment analysis was performed for the whole set of PFRGs, as well as for pro- and anti-fibrotic genes separately. PFRGs were enriched in processes such as proliferation, inflammation, immune functions and cancer. Regulation of proliferation enrichment was consistent across pro- and anti-fibrotic genes: pro-fibrotic genes were enriched for positive regulation and anti-fibrotic genes were enriched for negative regulation of proliferation (Table 3). Several aging-related pathways showed enrichment in pro-fibrotic genes, such as insulin resistance, stress response, PI3K-Akt, FoxO signaling pathways and apoptosis. These results highlight the association between pulmonary fibrosis and the aging process.

Table 3. Enriched Gene Ontology Biological Processes for PFRGs

All PFRGs	**Pro-fibrotic PFRGs**	**Anti-fibrotic PFRGs**
Regulation of proliferation	*Positive regulation of proliferation*	*Negative regulation of proliferation*
Cytokine signaling	*Cytokine signaling*	
Inflammation	*Inflammation*	
Immune function	*Immune function*	
Cancer	*Cancer*	*Cancer*
Reaction to pathogen	*Reaction to pathogen*	
Oxygen homeostasis	*Oxygen homeostasis*	
MAPK signaling pathway		*MAPK signaling pathway*
TNF signaling pathway	*TNF signaling pathway*	
Jak-STAT signaling pathway	*Jak-STAT signaling pathway*	
Asthma		
Aging		
	Insulin resistance	
	Stress response	
		Estrogen signaling pathway
		Response to mechanical stimulus
	PI3K-Akt signaling pathway	
	VEGF signaling pathway	
	FoxO signaling pathway	
	Apoptosis	

Next, we constructed a PPI network for the human ortholog proteins of mouse PFRGs (Fig. 11A) and found that 56.3% of PFRGs (107 nodes) form a continuous component. This percentage is extremely high compared to the expected percentage of genes forming a continuous network from randomly sampling 190 nodes from the interactome (Z-score of 5.36, Fig. 12B). In addition to being more interconnected than expected by chance, PFRGs also have a higher mean connectivity across the whole interactome (64.4), compared to the average connectivity of all genes (45.5) (Fig. 12C). Furthermore, by performing a Gene-Set Enrichment Analysis of all the genes in the interactome ranked by their degree, we found a highly significant enrichment among the highest connected genes for PFRGs (ES = 0.6, $p<0.05$) (Fig. 12B). Noteworthy, among the hubs in the PFRGs network are well-known aging-associated genes, such as AKT1, HIF1A, SIRT1, HSPA5.

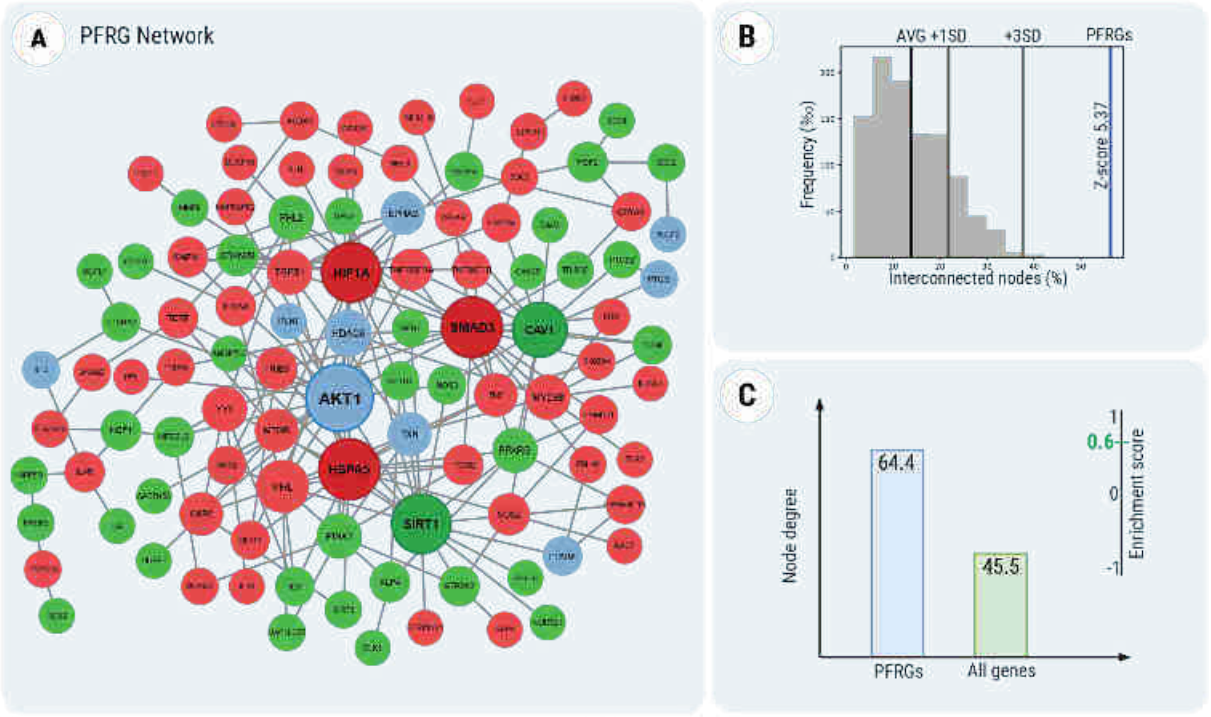

Figure 11. Network visualization of protein-protein interactions between PFRGs. (A) Largest continuous component of the protein-protein interactions networks for all PFRGs (n=107 nodes). The top 5% nodes with the highest degree are highlighted with bold labels. **(B)** Percentage of nodes forming the largest continuous connected component (percentage of interconnected nodes) for a number of nodes equal to the size of PFRGs gene set (n = 190), randomly sampled from the human interactome. The analysis for interconnectivity was repeated 1,000 times; the histogram shows the distribution of these 1,000 values that represent the percentage of interconnected nodes (distribution average 13.9%, SD: 7.9%). The vertical

lines depict the values for the mean of the distribution (AVG), as well as one standard deviation and three standard deviations from the mean. The blue line corresponds to the Z score of the PFRGs on this distribution. **(C)** Comparison of average degree in the human interactome (BioGRID v 3.5.188) for PFRGs (blue bar) and all the genes corresponding to the whole proteome (green bar). Figure adapted from (Toren et al., 2021), used under license CC BY 4.0.

2.6. Drug repurposing

One approach towards the identification of longevity-modulator drugs is to prioritize the molecules that induce a transcriptional profile that is opposite to the one associated with the aging process itself, i.e. drugs that could potentially reverse the transcriptional drift that occurs with aging. Among the drugs that target aging-related pathways, those that could be useful for cellular reprogramming constitute another promising approach for rejuvenation.

2.6.1. Drugs with potential to reverse the shift in transcriptional profile associated with neurodegenerative diseases

The similarities observed between the aging signature and the AD/PD signatures suggest that the shared transcriptional profiles point to a more vulnerable state and might have a role in the degenerative process. In order to identify chemicals with potential therapeutic use against neurodegeneration, we search for drugs that induce a transcriptional profile opposite to the one associated with pathological changes. Ideally, a therapeutic approach would be to fully reverse the transcriptome to a young state, but it is improbable to be achieved in practice. Instead, we propose to search for compounds that could potentially drive the system to a younger, healthier state.

We used the Connectivity Map tool (Subramanian et al., 2017) for our approach, an online tool that holds more than 1 million transcriptional profiles of approximately 20,000 compounds in 70 human cell lines, obtained through perturbation studies. This tool uses the GSEA method (Subramanian et al., 2005) in order to calculate a score for each drug, using the signature of up- and down-regulated genes given as input. A positive score shows that the drug has a similar profile to the input profile, whereas a negative score suggests an opposite profile.

The AD-cluster analysis revealed 15,076 significant drugs (FDR<0.05) with opposite profiles to the signature changes occurring in AD or similar aging states. We prioritized the most significant drugs with the highest negative scores and found, among the top 200, 9 drugs whose mechanisms have already been associated with aging-related processes, such as: modulation of inflammation pathways, through CC chemokine receptor antagonism (AMG-487) or lipoxygenase inhibition (diethylcarbamazine); apoptosis stimulation (BRD-K68144790) or inhibition of X-linked inhibitor of apoptosis (GDC-0152), MEK inhibition (selumetinib) - which can prevent or suppress cellular aging (Steelman et al., 2011), Heat Shock Proteins (HSPs) induction (homosalate) - which have a pro-longevity role and regulates cellular senescence and apoptosis (Tower, 2009), inhibition of mTOR (AZD-8055), modulation of PPAR proteins (Pioglitazone, Rupacarib) - which are involved in oxidative stress and energy metabolism (Erol, 2007).

The PD-cluster analysis revealed only 194 significant drugs (FDR<0.05) with opposite profiles to the PD signature. Among the top hits we also found 8 drugs already approved for the pathologies represented in the cluster, as well as other experimental drugs or compounds with similar mechanisms to the already approved ones, which might be promising new therapeutic agents. This analysis revealed as potential mechanisms: modulation of estrogen receptor (Raloxifen - approved for the treatment of osteoporosis and Bazedoxifene - a newer generation of modulators, approved for prevention of postmenopausal osteoporosis), anticholinergic drugs (Metixene - approved as antiparkinsonian, Solifenacin - approved for urinary incontinence, Mebeverine - approved as antispastic and Deltaline), dopamine receptor agonism (Metergoline) and phospholipase inhibition (Darapladib - an investigational drug for stabilization of atherosclerotic plaque).

2.6.2. Small molecules for cell reprogramming

Small molecules for cell reprogramming were curated from the peer-reviewed scientific literature and annotated with chemical properties from PubChem (Kim et al., 2021) and Human Metabolome Database (HMDB) (Wishart et al., 2018). The 92 compounds were classified, based on their role in reprogramming as inducers, enhancers, or, in some cases, both. Additionally, we curated a list of 10 cocktails including only combinations of drugs that together induce partial or total reprogramming, without requiring the presence of transcription factors.

These compounds can be divided into three main functional categories (signaling modifiers - mostly inhibitors of TGF□, epigenetic modifiers - methyltransferases and histone deacetylases, metabolic modifiers - inhibitors of GSK3), as well as a small fraction that don't belong to any of these three (Figure 12).

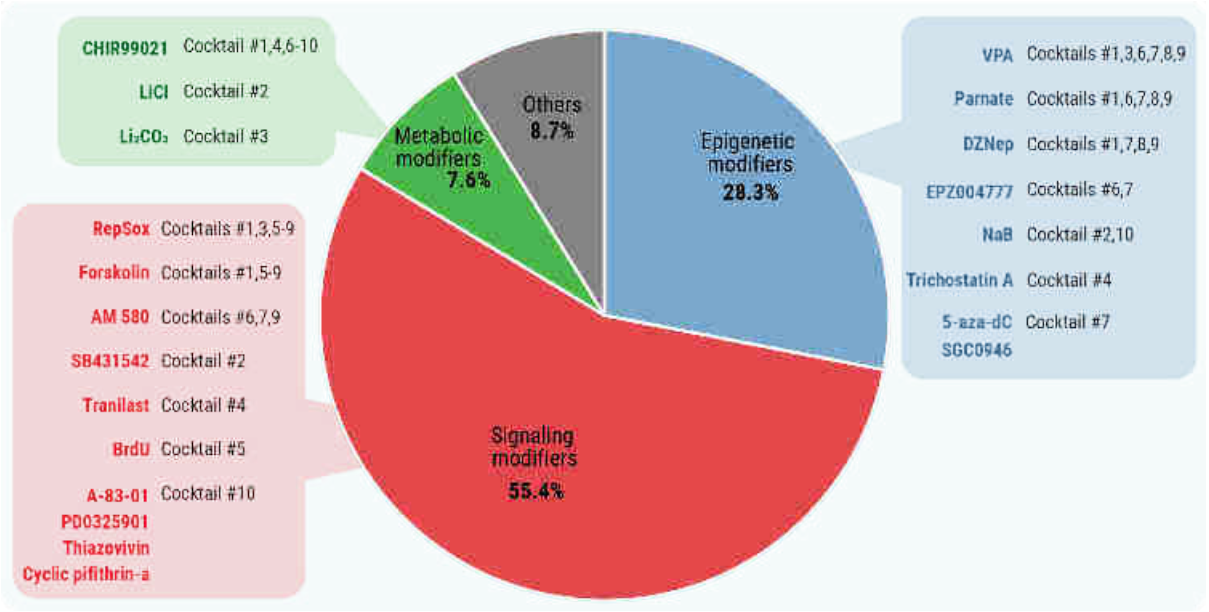

Figure 12. Distribution of the 92 enhancers/inducers of pluripotency based on the functional category. The chart depicts the percentage of the 92 drugs that fall under each category (signaling modifiers, epigenetic modifiers, metabolic modifiers and others). The side panels show only the drugs from the cocktails in these categories, together with the cocktail(s) to which they belong. Figure derived from (Knyazer et al., 2021), used under license CC BY 3.0.

In order to provide a systems biology view of the protein targets of the SMs, we constructed a PPI network of 991 proteins and 6,072 interactions. The network fits a scale-free structure, characteristic of biological networks (Fig. 13A), with the node degree following a power law distribution: $P(k) = 221 * k^{-1.16}$. Moreover, the networks of 991 proteins as well as each subnetwork of the 10 cocktails are more interconnected than expected by chance (Fig. 13B). Such high interconnectivity for all cocktails supports the notion that the cocktails are targeting a series of proteins that normally work together in achieving their function.

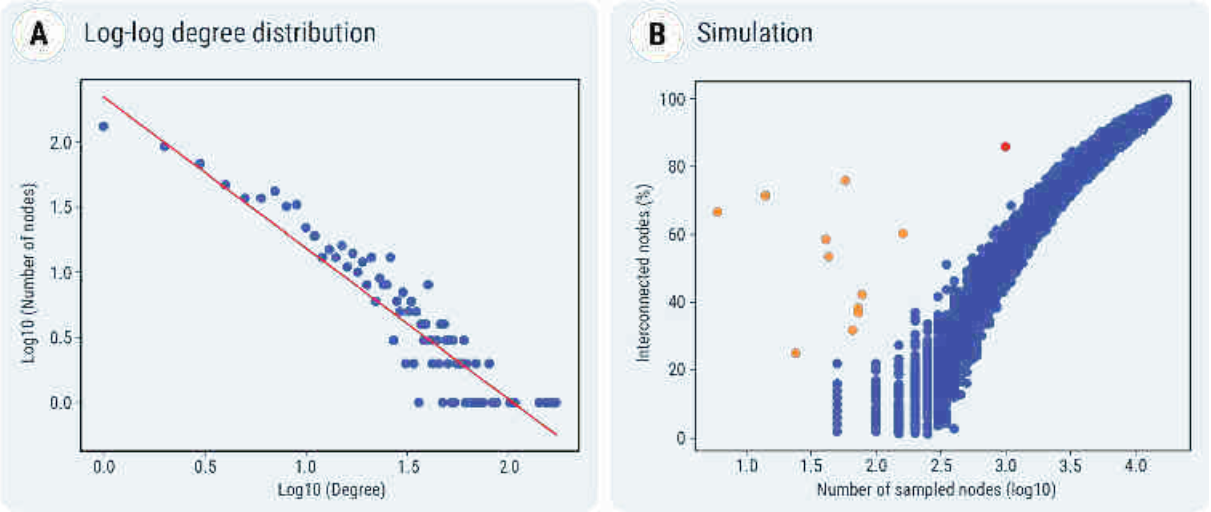

Figure 13. Protein-protein interactions network for protein targets of the small molecules that induce or enhance pluripotency. (A) Percentage of nodes forming the largest connected component in randomly sampled subnetworks from the interactome of various sizes. The node set size varies from 50 to 17,600, with a step of 50, represented in log scale on the X-axis. The orange points represent the interconnectivity observed for the PPINs of the 9 cocktails and the red point represents the interconnectivity observed for the network of 991 protein targets; **(B)** Scale-free fit for the network of 991 protein targets. The scatter plot represents the distribution of the degree in a logarithmic scale. The red line depicts the fit of the linear function that approximates the distribution (in the log-log scale). Figure derived from (Knyazer et al., 2021), used under license CC BY 3.0.

We performed a comparison between the targets of the 10 cocktails and the targets of Yamanaka's factors, both at the level of proteins and pathways. Interestingly, the overlap between protein targets was limited and non-significant for all cocktails, except for cocktail 7 (n=15, p=0.0033, Fig. 14A). However, at the pathway level, the overlap is significant and consistent for four cocktails and includes multiple cancer-related pathways (Figure 14B).

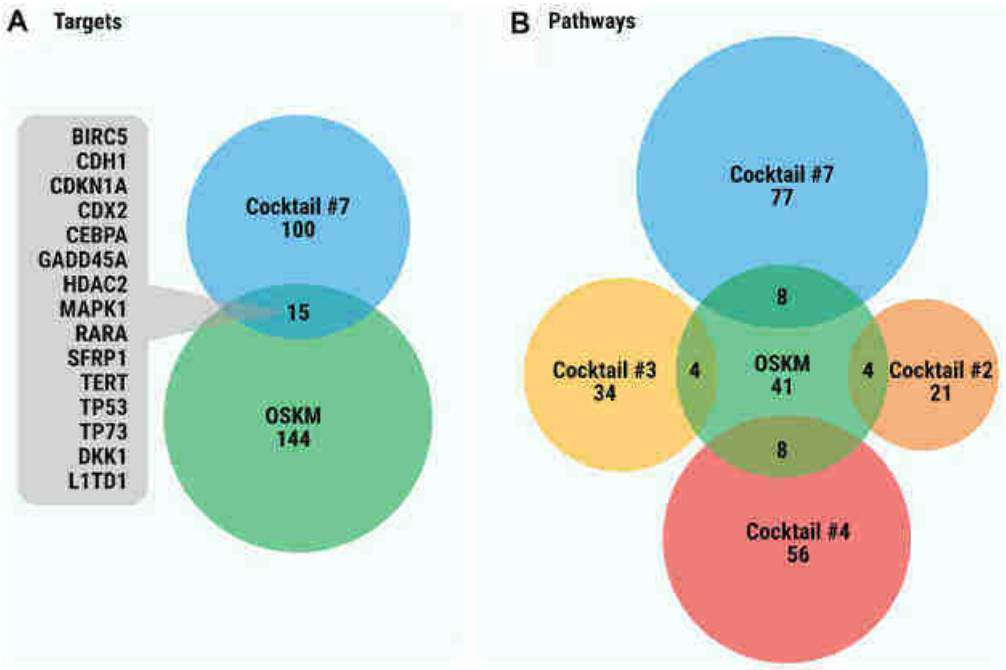

Figure 14. Venn diagram of intersection between (A) protein targets of cocktails and protein targets of OSKM transcription factors; **(B)** pathways enriched in protein targets of cocktails and pathways enriched in protein targets of OSKM. For simplification, the pathway overlaps between pairs of cocktails were not displayed in the figure. Figure derived from (Knyazer et al., 2021), used under license CC BY 3.0.

2.6.3. Drugs that induce pluripotency as potential agents against neurodegenerative pathologies

Next, using the previously described list of small molecules for cellular reprogramming, referred to as PASMs - "Pluripotency-associated small molecules", I prioritized genetic targets for the age-related diseases studied and investigated whether the drugs that induce cell rejuvenation could improve the neurodegenerative phenotype, based on a bioinformatics analysis of their gene targets.

The 10 PASM cocktails have a certain degree of overlap in constituent drugs. In addition, a larger number of small molecules and, consequently, a large number of targets used as input for a bioinformatics analysis would increase the probability of off-targets. Therefore, the analysis focused on the most “compact” cocktails, i.e. the smallest number of small molecules which can achieve reprogramming to the stage of neural progenitor cells. Three cocktails were selected: 1)Valproic acid, CHIR99021, RepSOX (VCR); 2)NaB, LiCl, SB431542 (NLS); 3)Trichostatin A, Li2CO3 / LiCl, Tranilast (TLT).

Several of these drugs are already known as longevity modulators, more precisely they increase the lifespan of model organisms. DrugAge (Barardo et al., 2017) reports that

valproic acid and lithium chloride increase the mean lifespan of *C. elegans* by 35% and 36%, respectively. Sodium butyrate increases the mean lifespan of *D. melanogaster* by 14% and trichostatin A showed a 22% increase in mean lifespan of nematodes.

Notably, none of the drugs in the PASMs list is FDA-approved for AD. Two of them are approved for other pathologies (valproic acid as anticonvulsant and lithium chloride as antipsychotic); trichostatin A and tranilast have therapeutic potential in humans, but are not approved; and the remaining drugs do not have any reported human use. The overlap between each cocktail's protein targets and the protein targets of the approved AD drugs is small, but statistically significant for all of them (Fig, 15A,B,C). The existence of common targets shows potential for identifying a new drug. Figure 15D highlights the overlap between targets of these three cocktails.

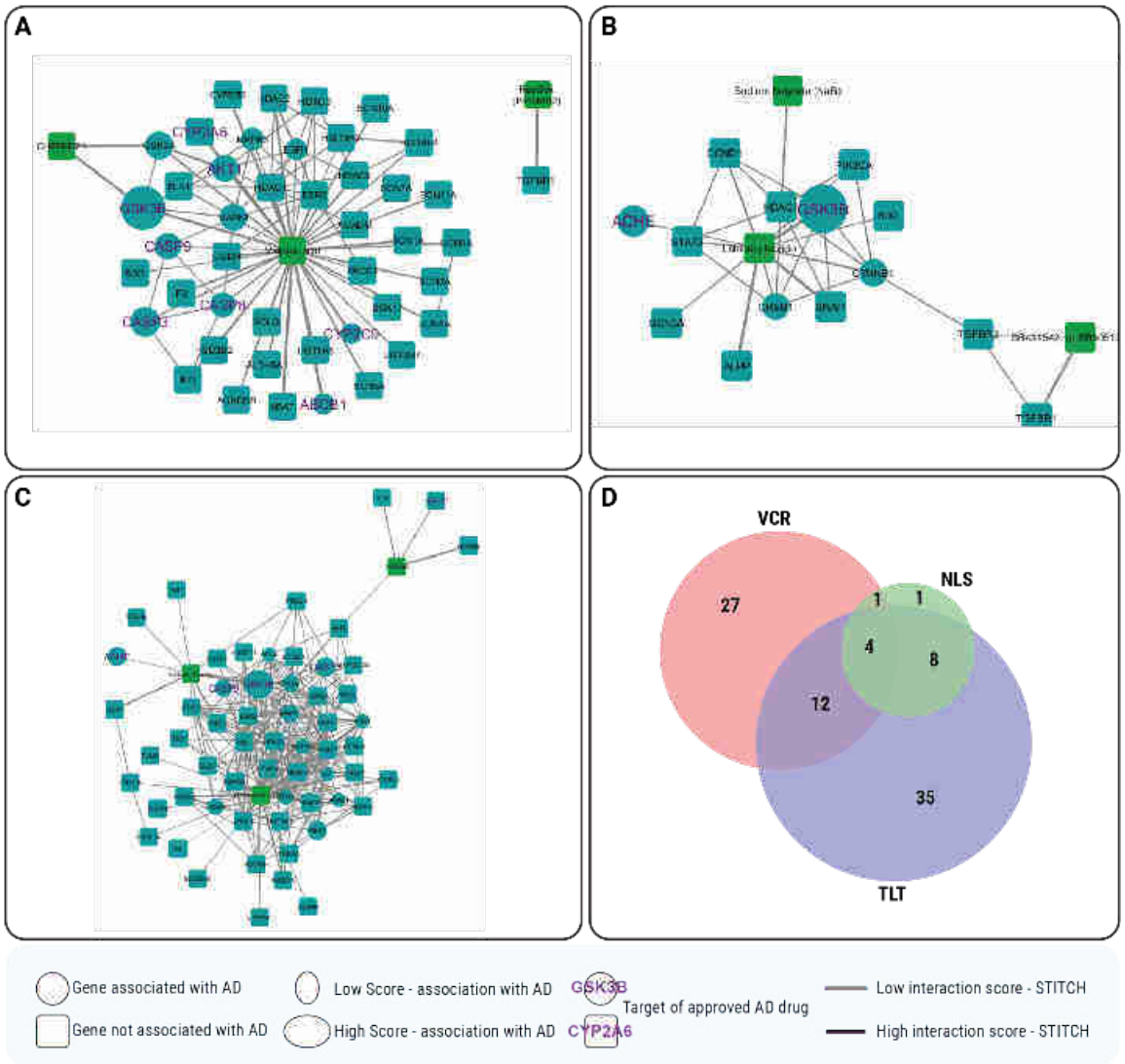

Figure 15. PASMs in the three selected cocktails and their targets: **A.** Cocktail VCR: Valproic acid, CHIR99021, RepSOX; **B**. Cocktail NLS: NaB, LiCl, SB431542; **C**. Cocktail TLT:

Trichostatin A, LiCl, Tranilast. **D**. Venn diagram of common gene targets between the three cocktails

The network analysis of drugs and proteins targets suggests a potential effect of PASMs as AD modulators (Fig. 15 A,B,C). The PASMs target some genes that are already known to be involved in AD-related pathology or genes that pertain to a potential AD modulatory mechanism. Among these targets, GSK3B, ACHE and AKT1 are all targets of already approved drugs. Based on the direction of interaction between the FDA-approved drugs and the proteins coded by these three genes, a potential therapeutic approach would involve downregulating GSK3B and ACHE and upregulating AKT1.

3. Final remarks

This work provides a systems biology approach to the study of aging and age-related diseases. Using bioinformatics methods pertaining to network biology and meta-analyses, I explored the molecular mechanisms of aging and ARDs, as well as the shared signatures and prioritized targets and drugs that can be repurposed as aging modulators.

One important achievement is the construction of the SynergyAge database, the first of its kind, that holds experimentally validated multiple genetic interventions on longevity-associated genes. Moreover, I proposed definitions for the interactions between two genes and novel ones for the more complex interactions between at least three genes. The SynergyAge database supports computational predictions of new genetic combinations, as demonstrated by our proposed (and validated) double mutant *odr-3;ife-2*, representative of an additive combination and experimentally validated by my colleagues in the lab.

Meta-analyses of aging and the selected age-related diseases highlighted common mechanisms that were grouped into two major clusters of transcriptional drifts. This finding was supported by a Connectivity Map analysis using these common signatures, which identified potential drugs that are involved in aging processes, already approved for ARDs or similar to approved drugs.

Another approach for drug repurposing was to choose drug combinations from the list of drug cocktails that induce partial cellular reprogramming. Mixed drug-protein networks were built for three cocktails, that were selected in order to maximize the age-related targets and minimize the off-targets. These cocktails show high potential as anti-neurodegenerative

agents, given the direction of drug-protein interactions and the associations of the protein targets with AD.

List of publications and presentations

Publications:

1. **Bunu G***, Toren D*, Ion CF, Barardo D, Sârghie L, Grigore LG, de Magalhães JP, Fraifeld V, Tacutu R. "SynergyAge, a curated database for synergistic and antagonistic interactions of longevity-associated genes", *Scientific Data*, 7:366 (2020), https://doi.org/10.1038/s41597-020-00710-z
2. Knyazer A*, **Bunu G***, Toren D, Bucaciuc Mracica T, Segev Y, Wolfson M, Muradian K, Tacutu R, Fraifeld V. "Small molecules for cell reprogramming: a systems biology analysis", *Aging (Albany NY)*, 13:25739-25762 (2021), https://doi.org/10.18632/aging.203791
3. Toren D, Yanai H, Abu Taha R, **Bunu G**, Ursu E, Ziesche R, Tacutu R, Fraifeld V. "Systems biology analysis of lung fibrosis-related genes in the bleomycin mouse model", *Scientific Reports*, 11:19269 (2021), https://doi.org/10.1038/s41598-021-98674-6
4. Matei IV, Samukange VNC, **Bunu G**, Toren D, Ghenea S, Tacutu R. "Knock-down of odr-3 and ife-2 additively extends lifespan and healthspan in C. elegans", *Aging (Albany NY)*, 13:21040-21065 (2021), https://doi.org/10.18632/aging.203518
5. Tacutu, R., Toren, D., Ursu, E., **Bunu, G**., Mracica, T.B. (2020). Healthy Biological Systems. In: Sholl, J., Rattan, S.I. (eds) Explaining Health Across the Sciences. *Healthy Ageing and Longevity*, vol 12. Springer, Cham. https://doi.org/10.1007/978-3-030-52663-4_5 (book chapter)
6. **Bunu G**, Toren D, Ursu E, Ghenea S, Fraifeld V, Tacutu R. "Drug prediction for reversing AD/PD transcriptional profiles using an aging of systems-centric approach", bioRxiv 2022.11.01.514657, https://doi.org/10.1101/2022.11.01.514657

* shared first co-authorship

Oral presentations

1. Bunu G, „SynergyAge: A Curated Database for Interactions of Longevity Genes", **Ending Age-Related Diseases 2020** - August 2020 (online)

2. Bunu G, ”Synergism and antagonism in aging”, **The Annual International Conference of the Romanian Society for Biochemistry & Molecular Biology**, September 2019, Iași, Romania

Poster presentations

1. Bunu G, Ion C, Tăcutu R, “Analysis of synergism and antagonism in aging”, **International Perspectives on Geroscience”** Israel, September 2019 - poster
2. Bunu G, Ion C, Tăcutu R, “Synergistic and antagonistic interventions between longevity genes - the SynergyAge database”, **International Conference on Aging and Disease**, October 2018, Nice, France (**Oustanding Poster Award**)
3. Bunu G, Ion C, Tăcutu R, “SynergyAge: a database of synergistic and antagonistic genes in aging research”, **The Annual International Conference of the Romanian Society for Biochemistry & Molecular Biology**, September 2018, Bucharest, Romania
4. Bunu G, Voinea A, Kulaga A, Constantinescu V, Craciun I, Ion C, Tăcutu R, “Gerontomics: a multi-omics prediction system for prioritization of gerontological interventions”, **The Annual International Conference of the Romanian Society for Biochemistry & Molecular Biology**, June 2017, Timisoara, Romania

Bibliography

Barardo, D., Thornton, D., Thoppil, H., Walsh, M., Sharifi, S., Ferreira, S., Anžič, A., Fernandes, M., Monteiro, P., Grum, T., et al. (2017). The DrugAge database of aging-related drugs. *Aging Cell* 16, 594–597. doi:10.1111/acel.12585.

Blagosklonny, M. V. (2012). Prospective treatment of age-related diseases by slowing down aging. *Am. J. Pathol.* 181, 1142–1146. doi:10.1016/j.ajpath.2012.06.024.

Bunu, G., Toren, D., Ion, C.-F., Barardo, D., Sârghie, L., Grigore, L. G., de Magalhães, J. P., Fraifeld, V. E., and Tacutu, R. (2020). SynergyAge, a curated database for synergistic and antagonistic interactions of longevity-associated genes. *Sci. Data* 7, 366. doi:10.1038/s41597-020-00710-z.

DeVito, L. M., Barzilai, N., Cuervo, A. M., Niedernhofer, L. J., Milman, S., Levine, M., Promislow, D., Ferrucci, L., Kuchel, G. A., Mannick, J., et al. (2022). Extending human healthspan and longevity: a symposium report. *Ann. N. Y. Acad. Sci.* 1507, 70–83. doi:10.1111/nyas.14681.

Erol, A. (2007). The functions of ppars in aging and longevity. *PPAR Res.* 2007, 39654. doi:10.1155/2007/39654.

Fernandes, M., Wan, C., Tacutu, R., Barardo, D., Rajput, A., Wang, J., Thoppil, H., Thornton, D., Yang, C., Freitas, A., et al. (2016). Systematic analysis of the gerontome reveals links between aging and age-related diseases. *Hum. Mol. Genet.* 25, 4804–4818. doi:10.1093/hmg/ddw307.

Fuentealba, M., Dönertaş, H. M., Williams, R., Labbadia, J., Thornton, J. M., and Partridge, L. (2019). Using the drug-protein interactome to identify anti-ageing compounds for humans. *PLoS Comput. Biol.* 15, e1006639. doi:10.1371/journal.pcbi.1006639.

Ge, Y., Zhou, M., Chen, C., Wu, X., and Wang, X. (2022). Role of AMPK mediated pathways in autophagy and aging. *Biochimie* 195, 100–113. doi:10.1016/j.biochi.2021.11.008.

Kim, S., Chen, J., Cheng, T., Gindulyte, A., He, J., He, S., Li, Q., Shoemaker, B. A., Thiessen, P. A., Yu, B., et al. (2021). PubChem in 2021: new data content and improved web interfaces. *Nucleic Acids Res.* 49, D1388–D1395. doi:10.1093/nar/gkaa971.

Knyazer, A., Bunu, G., Toren, D., Mracica, T. B., Segev, Y., Wolfson, M., Muradian, K. K., Tacutu, R., and Fraifeld, V. E. (2021). Small molecules for cell reprogramming: a systems biology analysis. *Aging (Albany NY)* 13, 25739–25762. doi:10.18632/aging.203791.

Liu, H., Guo, M., Xue, T., Guan, J., Luo, L., and Zhuang, Z. (2016). Screening lifespan-extending drugs in Caenorhabditis elegans via label propagation on drug-protein networks. *BMC Syst. Biol.* 10, 131. doi:10.1186/s12918-016-0362-4.

Matei, I. V., Samukange, V. N. C., Bunu, G., Toren, D., Ghenea, S., and Tacutu, R. (2021). Knock-down of odr-3 and ife-2 additively extends lifespan and healthspan in C. elegans. *Aging (Albany NY)* 13, 21040–21065. doi:10.18632/aging.203518.

Miller, J. A., Oldham, M. C., and Geschwind, D. H. (2008). A systems level analysis of transcriptional changes in Alzheimer's disease and normal aging. *J. Neurosci.* 28, 1410–1420. doi:10.1523/JNEUROSCI.4098-07.2008.

Oughtred, R., Stark, C., Breitkreutz, B.-J., Rust, J., Boucher, L., Chang, C., Kolas, N., O'Donnell, L., Leung, G., McAdam, R., et al. (2019). The BioGRID interaction database: 2019 update. *Nucleic Acids Res.* 47, D529–D541. doi:10.1093/nar/gky1079.

Steelman, L. S., Chappell, W. H., Abrams, S. L., Kempf, R. C., Long, J., Laidler, P., Mijatovic, S., Maksimovic-Ivanic, D., Stivala, F., Mazzarino, M. C., et al. (2011). Roles of the Raf/MEK/ERK and PI3K/PTEN/Akt/mTOR pathways in controlling growth and sensitivity to therapy-implications for cancer and aging. *Aging (Albany NY)* 3, 192–222.

Subramanian, A., Narayan, R., Corsello, S. M., Peck, D. D., Natoli, T. E., Lu, X., Gould, J., Davis, J. F., Tubelli, A. A., Asiedu, J. K., et al. (2017). A next generation connectivity map: L1000 platform and the first 1,000,000 profiles. *Cell* 171, 1437-1452.e17. doi:10.1016/j.cell.2017.10.049.

Subramanian, A., Tamayo, P., Mootha, V. K., Mukherjee, S., Ebert, B. L., Gillette, M. A., Paulovich, A., Pomeroy, S. L., Golub, T. R., Lander, E. S., et al. (2005). Gene set enrichment analysis: a knowledge-based approach for interpreting genome-wide expression profiles. *Proc Natl Acad Sci USA* 102, 15545–15550. doi:10.1073/pnas.0506580102.

Szklarczyk, D., Santos, A., von Mering, C., Jensen, L. J., Bork, P., and Kuhn, M. (2016). STITCH 5: augmenting protein-chemical interaction networks with tissue and affinity data. *Nucleic Acids Res.* 44, D380-4. doi:10.1093/nar/gkv1277.

Tacutu, R., Budovsky, A., Yanai, H., and Fraifeld, V. E. (2011). Molecular links between cellular senescence, longevity and age-related diseases - a systems biology perspective. *Aging (Albany NY)* 3, 1178–1191.

Tacutu, R., Thornton, D., Johnson, E., Budovsky, A., Barardo, D., Craig, T., Diana, E., Lehmann, G., Toren, D., Wang, J., et al. (2018). Human Ageing Genomic Resources: new and updated databases. *Nucleic Acids Res.* 46, D1083–D1090. doi:10.1093/nar/gkx1042.

Toren, D., Yanai, H., Abu Taha, R., Bunu, G., Ursu, E., Ziesche, R., Tacutu, R., and Fraifeld, V. E. (2021). Systems biology analysis of lung fibrosis-related genes in the bleomycin mouse model. *Sci. Rep.* 11, 19269. doi:10.1038/s41598-021-98674-6.

Tower, J. (2009). Hsps and aging. *Trends Endocrinol. Metab.* 20, 216–222. doi:10.1016/j.tem.2008.12.005.

Wishart, D. S., Feunang, Y. D., Marcu, A., Guo, A. C., Liang, K., Vázquez-Fresno, R., Sajed, T., Johnson, D., Li, C., Karu, N., et al. (2018). HMDB 4.0: the human metabolome database for 2018. *Nucleic Acids Res.* 46, D608–D617. doi:10.1093/nar/gkx1089.

Xie, E., Nadeem, U., Xie, B., D'Souza, M., Sulakhe, D., and Skondra, D. (2022). Using Computational Drug-Gene Analysis to Identify Novel Therapeutic Candidates for Retinal Neuroprotection. *Int. J. Mol. Sci.* 23. doi:10.3390/ijms232012648.

Xue, H., Xian, B., Dong, D., Xia, K., Zhu, S., Zhang, Z., Hou, L., Zhang, Q., Zhang, Y., and Han, J.-D. J. (2007). A modular network model of aging. *Mol. Syst. Biol.* 3, 147. doi:10.1038/msb4100189.

Zhang, Q., Nogales-Cadenas, R., Lin, J.-R., Zhang, W., Cai, Y., Vijg, J., and Zhang, Z. D. (2016). Systems-level analysis of human aging genes shed new light on mechanisms of aging. *Hum. Mol. Genet.* 25, 2934–2947. doi:10.1093/hmg/ddw145.